Pergamon

Tetrahedron 58 (2002) 815–824

TETRAHEDRON

Imprinting of specific molecular recognition sites in inorganic and organic thin layer membranes associated with ion-sensitive field-effect transistors

Maya Zayats, Michal Lahav, Andrei B. Kharitonov and Itamar Willner*

Institute of Chemistry, The Hebrew University of Jerusalem, Jerusalem 91904, Israel

Received 23 July 2001; revised 1 October 2001; accepted 2 October 2001

Abstract—Molecular recognition sites were imprinted in inorganic TiO_2 films, and acrylamide–acrylamidephenylboronic acid copolymer membranes, associated with ion-sensitive field-effect transistors, ISFETs, that act as transduction devices for the association of the substrates to the imprinted membranes. Molecular structures of carboxylic acids, e.g. 4-chlorophenoxyacetic acid (**1**), 2,4-dichlorophenoxyacetic acid (**2**), fumaric acid (**3**), and maleic acid (**4**), are imprinted in TiO_2 films. The imprinted sites reveal high specificity, and substrates, structurally-related to the imprinted compounds are fully differentiated by the imprinted membranes. The specificity of the imprinted sites originates from the complementary structural fitting and ligation of the guest carboxylic acid residues to the Ti(IV)–OH sites in the host carboxylic acids to the imprinted cavities. An acrylamide–acrylamidephenylboronic acid copolymer acts as a functional polymer for the imprinting of nucleotides, e.g. adenosine 5′-monophosphate, AMP, (**7**), guanosine 5′-monophosphate, GMP, (**8**), or cytosine 5′-monophosphate, CMP, (**9**). The specificity of the imprinted nucleotide sites originates from the cooperative binding interactions between the nucleotides and the boronic acid ligand and acrylamide H-bonds. The detection regions and sensitivities for sensing of the different substrates by the functional polymers are determined.

Imprinting of molecular recognition sites in bulk polymers or inorganic matrices has been a subject of extensive research efforts in the last two decades.[1,2] Two general strategies have been suggested to generate molecular imprinted recognition sites. One method includes the polymerization of monomer units complementary to the chemical functionalities in a substrate molecule, followed by the physical removal of the imprinted substrate by a washing process.[3,4] The second approach includes the covalent attachment[5] or coordination[6] of the substrate to polymerizable monomer units. Polymerization of the functionalized substrate molecule in the presence of another monomer yields a substrate-functionalized copolymer. Cleavage of the polymer-linked substrate yields the imprinted sites. Molecular imprinted organic polymers or inorganic polymers such as silica gels[7] or TiO_2[8] were prepared with structural[9] and chiral[10] selectivities. The different imprinted matrices were used for chromatographic separations[11,12] and for selective reactions in the imprinted cavities.[13] The use of membranes that include imprinted molecular recognition sites is particularly tempting for selective sensing applications. Although different sensors based on the imprinting process have been reported,[14] the methods suffer from basic limitations: (i) the imprinted polymer matrices are usually thick, and the number of recognition sites per unit volume of the polymer is relatively low. This introduces diffusion barriers for the substrate, resulting in slow response-times and moderate sensitivities and (ii) it is difficult to electrically communicate the molecular recognition sites with electronic transducers, and thus the electronic transduction of the sensing events is difficult. Indeed, most of the sensor devices based on molecular imprinted matrices are either optical (include a chromogenic marker)[15] or include microgravimetric, quartz-crystal microbalance (QCM)[16,17] analyses of the substrates.

Recently, an approach to generate molecular imprinted sites in a two-dimensional monolayer array associated with a surface was reported.[18,19] Imprinting of molecular recognition sites was accomplished by photochemical cleavage of the imprinted substrate from the monolayer assembly[18] or by the incorporation of a specific binding element in the monolayer.[19] The close proximity between the electrode and the imprinted sites in these systems enabled the electrochemical transduction (amperometric or capacitance signals) of the formation of the affinity complexes between the substrate and the imprinted sites.

Recently, we have reported on the assembly of TiO_2 thin films on an ISFET, and in a preliminary study we reported on the selective analysis of chloroaromatic acids.[20] In the present report we describe a comprehensive study on the

Keywords: ion-sensitive field-effect transistors; molecular recognition sites; molecular imprinting; sensor; ISFET.

* Corresponding author. Tel.: +972-2-6585272; fax: +972-2-6527715; e-mail: willnea@vms.huji.ac.il

0040–4020/02/$ - see front matter
PII: S0040-4020(01)01112-7

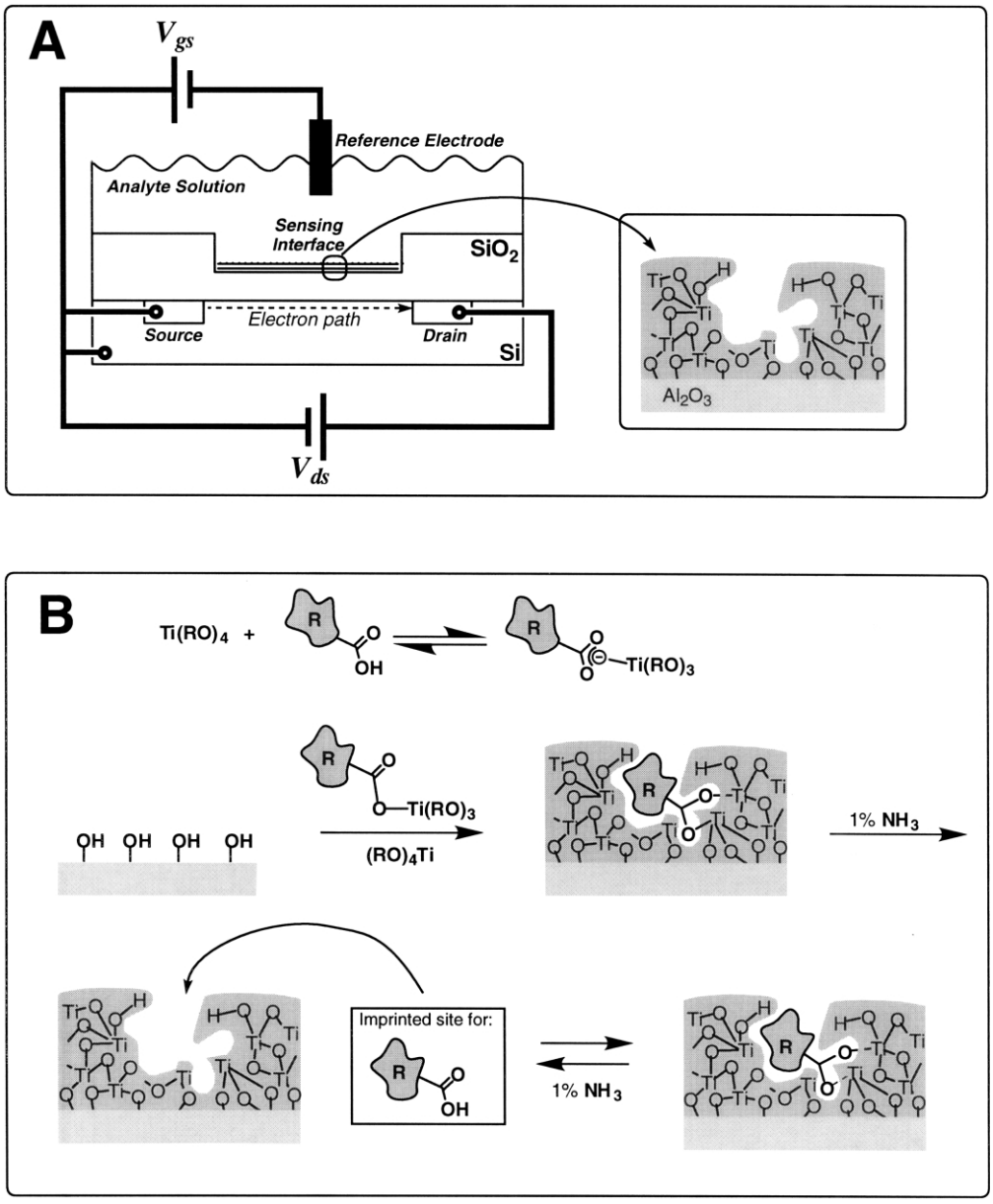

Scheme 1. (A) Schematic configuration of the molecular-imprinted ISFET device. (B) Preparation of molecular-imprinted sites for carboxylic acids in a TiO_2 thin film acting as the sensing interface on the ISFET gate.

imprinting of molecular recognition sites in thin inorganic or organic films associated with ISFETs and piezoelectric quartz-crystals. We describe a novel method for the imprinting of molecular recognition sites for nucleotides. We also demonstrate significant structural selectivity upon imprinting of molecular recognition sites in TiO_2 membranes.

1. Results and discussion

Carboxylic acids were imprinted in TiO_2 films associated with the gate surface of an ISFET device as shown in Scheme 1(A). Hydrolytic polymerization of the Ti(IV) carboxylate or tributoxide complex on the SiO_2 surface of the ISFET followed by the removal of the carboxylate in the presence of ammonia, yields imprinted sites in the resulting TiO_2 film. Scheme 1(B) shows the schematic configuration of the ISFET device that includes the imprinted membrane as sensing interface. Deprotonation of the hydroxylated Ti–OH interface controls the charge and, respectively, the potential of the gate. That is, at a certain gate potential, and upon the application of the appropriate potential between the source and drain of the ISFET, a constant current flows between the source and drain. Binding of the host–substrate to the imprinted sites generates the Ti(IV)–carboxylate complex. This depletes the hydroxyl functionalities and alters the gate potential. In order to retain the current between the source and drain of the FET, the gate potential must be compensated by an external voltage, V_{gs} (applied between the reference electrode and the source). Provided the imprinted sites are selectively occupied by the imprinted substrate the bulk concentration of the substrate controls the occupation of the imprinted membrane, and thus the gate potential.

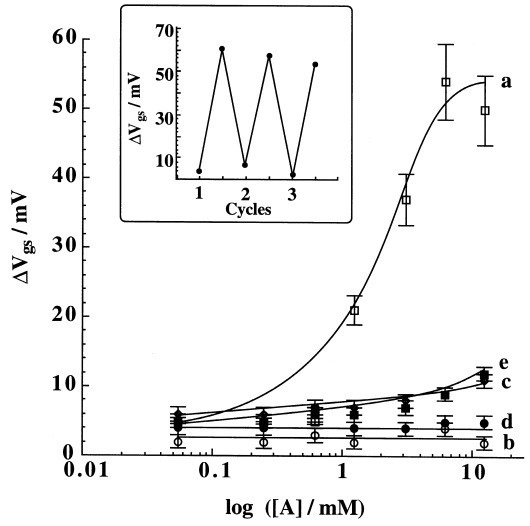

Figure 1. The gate–source potential changes, (ΔV_{gs}) of the device upon: (a) interaction of the device with the (**1**)-imprinted TiO_2 film with varying concentrations of (**1**); (b) interaction of the device which includes a non-imprinted TiO_2 film with varying concentrations of (**1**); (c)–(e) interaction of the (**1**)-imprinted device with varying concentrations of 2,4-dichlorophenoxyacetic acid (**2**), cinnamic acid and benzoic acid, respectively. Inset: cyclic analysis of (**1**) by the (**1**)-imprinted TiO_2 film-functionalized ISFET device. Upper points correspond to the response of the device after interaction with (**1**) (6.25×10^{-3} M). Lower points correspond to the response of the device after the rinsing of the membrane and the depletion of the bound analyte with ammonia solution, 1% (v/v), followed by rinsing with 0.1 M phosphate buffer solution, pH=7.2. The Na^+-salt of the different acids were used in the different experiments. A=Analysed carboxylic acid.

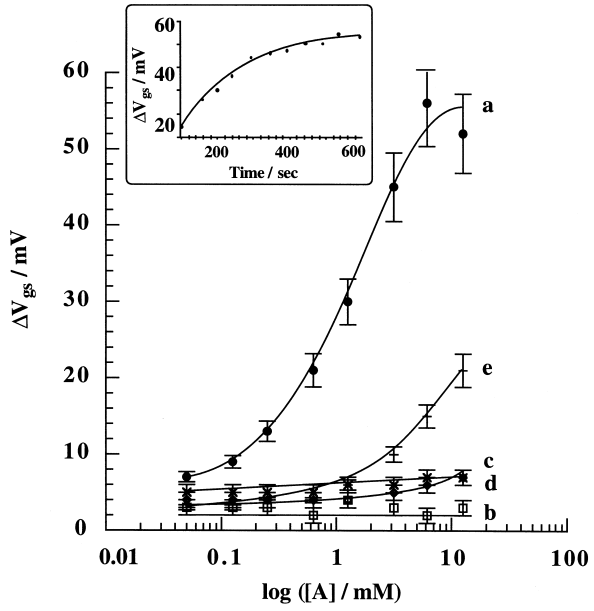

Figure 2. The gate–source potential changes, (ΔV_{gs}) of the ISFET upon: (a) interaction of the (**2**)-imprinted TiO_2 film sensing interface with varying concentrations of (**2**); (b) interaction of the device that includes a non-imprinted TiO_2 film with varying concentrations of (**2**); (c)–(e) treatment of the (**2**)-imprinted sensing interface with varying concentrations of (**1**), cinnamic acid and benzoic acid, respectively. Inset: time-dependent development of the gate–source potential of the ISFET functionalized with the (**2**)-imprinted TiO_2 film upon the sensing (**2**), 1×10^{-4} M.

Chloroaromatic acids such as 4-chlorophenoxyacetic acid (**1**) or 2,4-dichlorophenoxyacetic acid (**2**) act as herbicides and are common ground, water and food contaminants. Previous studies reported on the imprint of molecular recognition sites for (**1**) and (**2**) in poly(ethyleneglycol dimethacrylate-co-4-vinylpyridine) or poly(trimethylolpropane trimethacrylate-co-4-vinylpyridine) polymer matrices and their analysis by means of fluorescene immunoassays,[21a] differential-pulse voltammetry on screen-printed electrodes,[21b] infrared evanescent wave spectroscopy,[21c] and colorimetric and chemiluminescence assays.[21d] We have generated imprinted TiO_2 membranes for (**1**) or (**2**) on the ISFET device. Fig. 1, curve (a), shows the analysis of (**1**) by the 4-chlorophenoxyacetic acid imprinted ISFET device. The substrate is analyzed with the sensitivity corresponding to 38 mV/dec and the lower detection limit of $(5\pm2)\times10^{-4}$ M. By rinsing the ISFET device with a 1% NH_3 solution, the sensing membrane can be regenerated, and (**1**) can be re-analyzed, Fig. 1, inset. The analysis of 4-chlorophenoxyacetic acid by the (**1**)-imprinted membrane is specific. A TiO_2 membrane which does not include any imprinted sites, assembled on the gate interface of the ISFET device by the hydrolytic polymerization of Ti(IV)–tetrabutoxide, does not yield a functional membrane for the analysis of (**1**), Fig. 1, curve (b). Similarly, the related aromatic acids, 2,4-dichlorophenoxyacetic acid, cinnamic acid and benzoic acid are not sensed by the (**1**)-imprinted TiO_2 membrane on the ISFET, Fig. 1, curves (c)–(e), respectively. Fig. 2 shows the analysis of 2,4-dichlorophenoxyacetic acid (**2**) by the (**2**)-imprinted TiO_2 membrane assembled on the ISFET device. It is clear that 2,4-dichlorophenoxyacetic acid is sensed by the (**2**)-imprinted membrane, Fig. 2, curve (a). The substrate is sensed in the concentration range of 0.1–9.0 mM with the sensitivity corresponding to 28 mV/dec, and the lower detection limit of $(5\pm0.2)\times10^{-5}$ M. Fig. 2, inset shows the equilibration time of the device upon the analysis of (**2**). The equilibration time, $\tau_{95\%}$ corresponds to ca. 5 min, ($\tau_{95\%}$ corresponds to the time-interval needed to reach 95% of the saturation value). A non-imprinted TiO_2 membrane assembled on the gate interface by the hydrolysis of Ti(IV)–tetrabutoxide is inactive in the analysis of (**2**), Fig. 2, curve (b). The (**2**)-imprinted TiO_2 membrane reveals significant selectivity. The structurally related aromatic acids 4-chlorophenoxyacetic acid (**1**), and cinnamic acid are not sensed by the (**2**)-imprinted ISFET device, Fig. 2, curves (c) and (d), respectively. The (**2**) imprinted ISFET device, however, yields a low signal in the presence of a high concentration of benzoic acid (in the concentration range of 1–10 mM the slope of the calibration curve is 18 mV/dec). The differentiation of the chloroaromatic acids (**1**) and (**2**) by the (**1**)- or (**2**)-imprinted membranes is significant. The lack of interaction of the (**1**)-imprinted membrane with (**2**) may be attributed to the cavity dimensions of the (**1**)-imprinted interface that cannot accommodate the larger 2,4-dichlorophenoxyacetic acid (**2**). The differentiation of the 4-chlorophenoxyacetic acid (**1**) by the (**2**)-imprinted ISFET device is, however, of further interest since (**1**) may structurally fit the larger 2,4-dichlorophenoxyacetic acid-imprinted cavity. To explain the observed sensing specificity we refer to Scheme 1 that outlines the mechanism of association of the guest substrate to the imprinted sites. The binding of the carboxylic acid to the imprinted site requires the structural fit of the acid to the imprinted polymeric contour and the additional covalent substitution of the Ti(IV)–OH

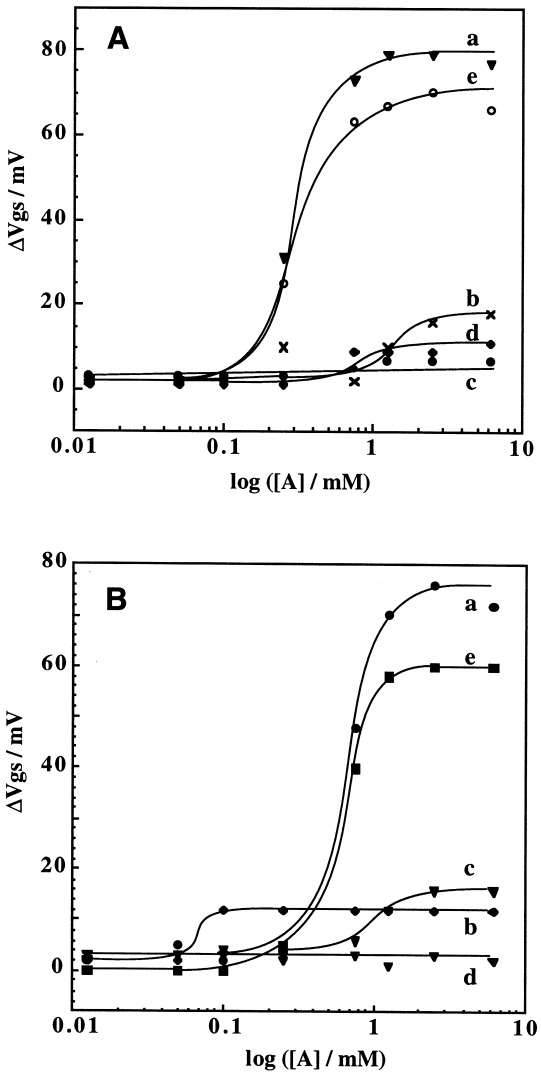

Figure 3. (A) The gate–source potential changes, (ΔV_{gs}) of the ISFET functionalized with the (**3**)-imprinted TiO_2 membrane upon: (a) interaction with variable concentrations of (**3**); (b)–(d) interaction with variable concentrations of maleic acid (**4**), acetylene dicarboxylic acid (**5**), and succinic acid (**6**), respectively; (e) the response of the (**3**)-imprinted sensing interface to (**3**) after 10 days of the operation. (B) The gate–source potential changes, (ΔV_{gs}) of the ISFET that includes the (**4**)-imprinted TiO_2 film upon: (a) interaction with varying concentrations of (**4**); (b)–(d) treatment with varying concentrations of fumaric acid (**3**), acetylene dicarboxylic acid (**5**), and succinic acid (**6**), respectively; (e) the response of the device that includes the (**4**)-imprinted TiO_2 film upon the sensing of (**4**) after 10 days of the operation.

functionality with the carboxylate group. These two binding interactions act synergetically in the association of the imprinted substrate to the functional cavities. Thus, although the (**2**)-imprinted membrane includes cavities that structurally may accommodate (**1**), the cavities lack the appropriate geometry that enables the simultaneous association to the cavities and the substitution of the Ti(IV)–OH sites by the carboxylate groups. The imprinted TiO_2 membranes reveal high stability towards the sensing of the imprinted substrates. We find that the imprinted membranes are stable for at least 1 month under continuous operating conditions. After 1 month of operation of the sensing devices we observe a 8–10% decrease in the sensitivity of the device. This might originate from the partial physical detachment of the membrane from the gate subjected to regeneration and rinsing cycles under continuous operation conditions, or to the partial degradation of the imprinted sites.[22]

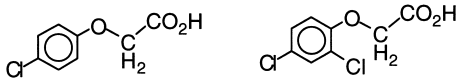

(**1**) (**2**)

The structural selectivity of imprinted molecular recognition sites for carboxylic acids in TiO_2 films is further emphasized by the generation of specific cavities for low molecular weight dicarboxylic acids, including *cis*/*trans* isomers. Fig. 3(A), curve (a), shows the response of a fumaric acid, (**3**) imprinted membrane associated with an ISFET device upon the analysis of (**3**). Fumaric acid is sensed in the concentration range of 0.08–1 mM with the sensitivity corresponding to 75±3 mV/dec. The lower detection limit for the analysis of (**3**) is 0.15 mM. The (**3**)-imprinted membrane is almost insensitive towards the analysis of the structurally related dicarboxylic acids such as maleic acid (**4**), acetylene dicarboxylic acid (**5**), and succinic acid (**6**), Fig. 3(A), curves (b)–(d), respectively. The resulting membrane reveals significant stability under continuous operation, and the response of the device after 10 days of operation is depicted in Fig. 3(A), curve (e). After this time-interval the sensor reveals the sensitivity of 65±2 mV/dec without changing the lower detection limit. The analysis of maleic acid (**4**), by the (**4**)-imprinted TiO_2-membrane associated with the ISFET device is shown in Fig. 3(B), curve (a). The imprinted substrate is sensed with the sensitivity of 70±2 mV/dec (concentration range of 0.2–3.0 mM), and the detection limit of 0.25 mM. Again, the imprinted membrane reveals specificity towards the imprinted substrate, and the structurally related substrates, fumaric acid (**3**), acetylene dicarboxylic acid (**5**), and succinic acid (**6**), are not detected by the (**4**)-imprinted membrane, Fig. 3(B), curves (b)–(d), respectively. Also, the (**4**)-imprinted membrane reveals high stability, and its sensitivity decreases by ca. 17% after 10 days of operation, Fig. 3(B), curve (e). Since the activity of functionalized ISFET device is retained under non-operating conditions, the partial degradation is attributed to the physical removal of parts of the membrane under continuous operation.

(**3**) (**4**)

(**5**) (**6**)

The latter C_4-dicarboxylic acid systems are interesting as they demonstrate that specific recognition sites, and molecular contours can be generated for low molecular weight substances of limited steric shape. The significant separation of the unsaturated acids (**3**) and (**4**) by the respective imprinted membranes is attributed to polymer contours and cavity structures dictated by the Ti(IV)–carboxylate

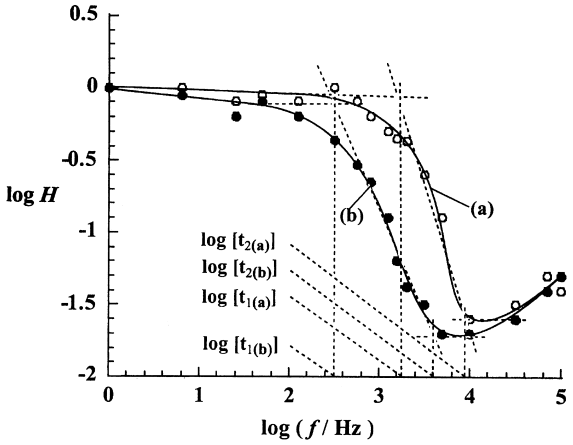

Figure 4. Transconductance curves corresponding to (a) the bare ISFET; (b) the TiO_2 film-functionalized ISFET device. Using the derived τ_1 and τ_2 values and Eqs. (1)–(3), the TiO_2 film thickness was estimated to be 85 ± 10 μm.

groups linked to the dicarboxylic acid functional groups of the substrate. In this context, it is important to mention the full differentiation of succinic acid (**6**) by the (**3**) and (**4**)-imprinted membranes. One would expect that the free C_2–C_3 bond-rotation would enable the association of a distorted succinic acid conformer to the imprinted sites. The experimental results clearly indicate that such binding of (**6**) does not occur. This complete steric differentiation of the imprinted sites is attributed to the fact that two complementary interactions operate in the specific binding of the substrate to the imprinted cavities. These include the cavity steric dimensions and the structural orientations of the carboxylate residues that form covalent bonds with the Ti(IV)–OH sites. The structural elongation of the sp^3-saturated dicarboxylic acid (**6**), prevents its binding to the sp^2 or sp-dicarboxylic acid confined structures.

An attempt was made to characterize the sensing interface and the imprinted sites in the film. The film thickness was determined by the use of impedance spectroscopy measurements on the modified gate interface.[23,24] The impedance features of the gate interface are controlled by the chemical composition of the modified gate.[23ac,24] In a recent study[25] we suggested to use impedance spectroscopy measurements on a functionalized gate as a method to evaluate the thickness of chemically assembled thin films on the gate surface. According to this method, the transconductance functions of the systems are recorded at variable applied frequencies and the time-constants, τ_1 (Eq. (1)), and τ_2 (Eq. (2)) are extracted from the curves, cf. Fig. 4. Using the time-constants, the resistance of the TiO_2 membrane, R_{mem}, and the capacitance of the TiO_2 film, C_{mem}, are determined. The value C_{ox} corresponds to the capacitance of the Al_2O_3 interface on which the TiO_2 film is assembled. From these values, the film thickness, δ_{mem}, is determined by using Eq. (3), where ϵ_o and ϵ_{mem} are dielectric constants of the vacuum ($\epsilon_o=8.85\times10^{-12}$ F/m) and the dielectric constant of the membrane, respectively, and A is the gate area.

$$\tau_1 = R_{mem}(C_{mem} + C_{ox}) \approx R_{mem}C_{ox} \quad (1)$$

$$\tau_2 = R_{mem}C_{mem} \quad (2)$$

$$C_{mem} = \frac{\epsilon_o \epsilon_{mem} A}{\delta_{mem}} \quad (3)$$

Fig. 4 shows the transconductance curves at variable frequencies corresponding to the bare ISFET device, curve (a), and the TiO_2 film-functionalized gate, curve (b). Using the derived C_{mem} and $\epsilon_{mem}\approx10$, we estimate the TiO_2 film thickness to be 85 ± 10 μm.

In order to further characterize the sensing interface associated with the gate, we attempted to estimate the number of imprinted sites in the sensing membrane. Towards this goal

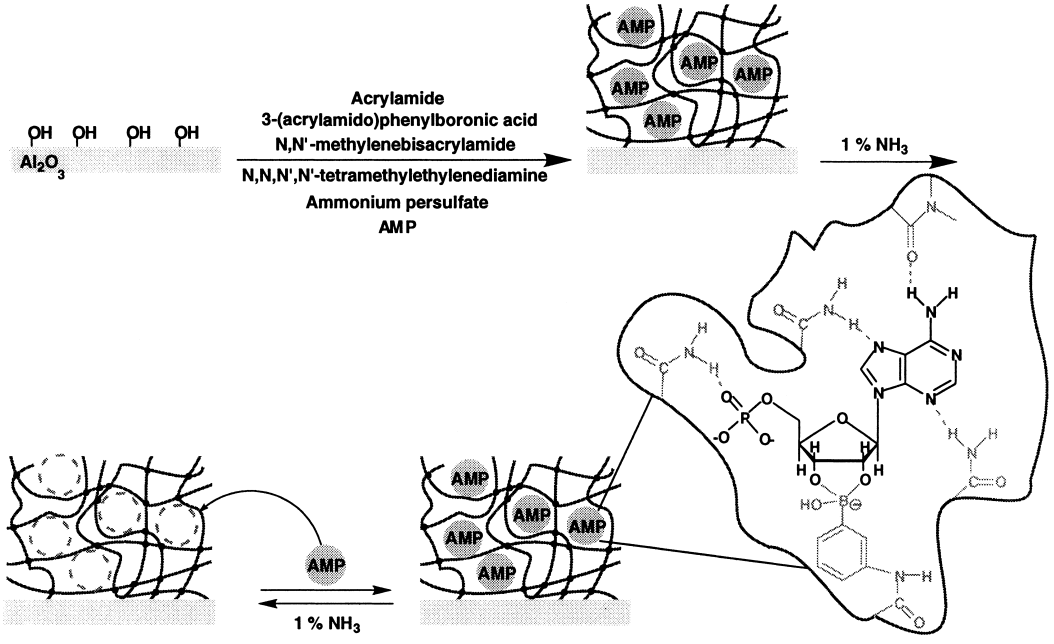

Scheme 2. Preparation of acrylamide–acrylamidephenylboronic acid copolymer with embedded imprinted sites for nucleotides.

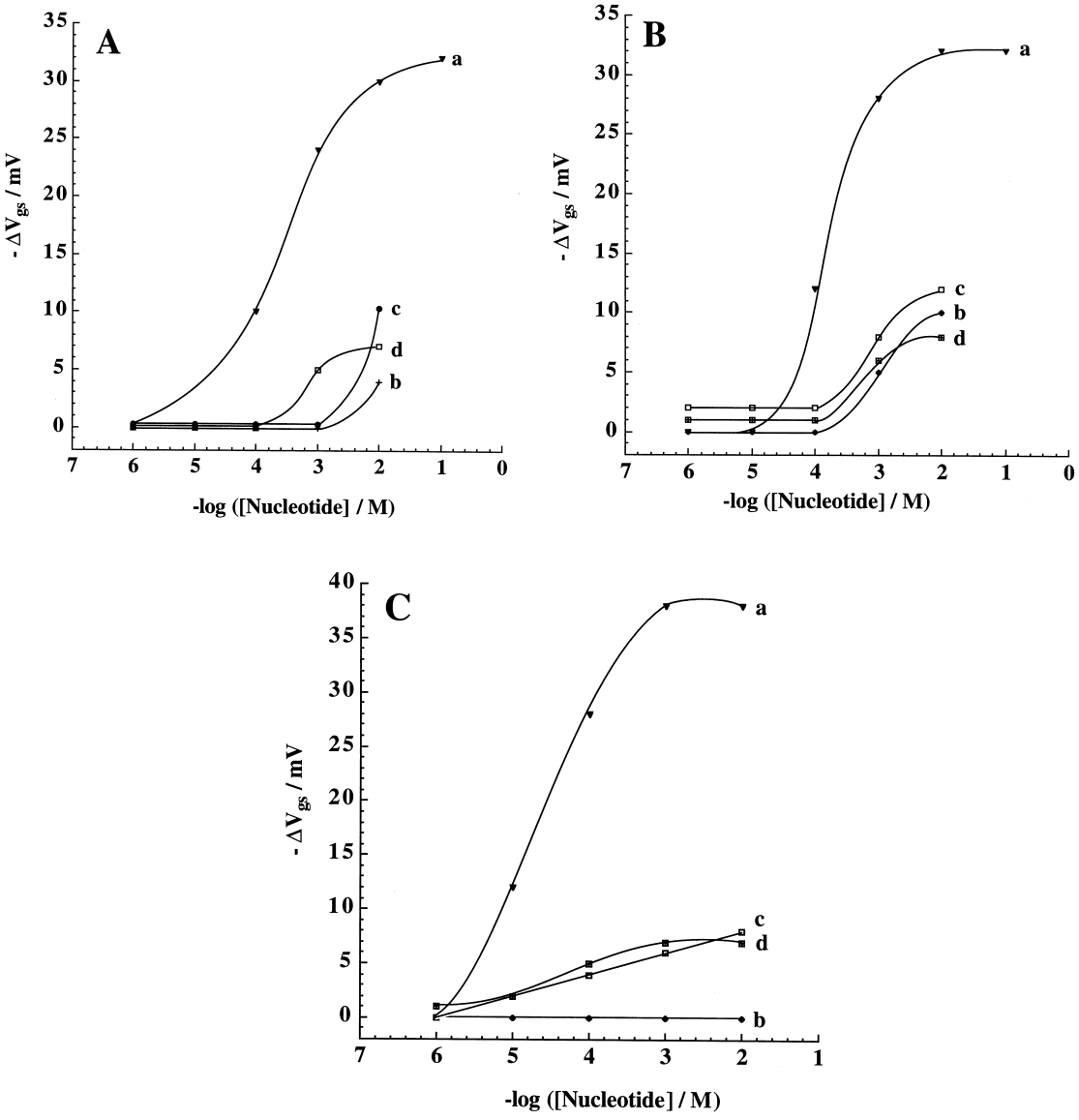

Figure 5. (A) The gate–source potential change of the ISFET device functionalized with the AMP-imprinted acrylamide–acrylamidephenylboronic acid copolymer upon the sensing of: (a) varying concentrations of AMP (**7**); (b),(c) varying concentrations of GMP (**8**) and CMP (**9**), respectively; (d) response of the ISFET functionalized with the non-imprinted acrylamide–acrylamidephenylboronic acid copolymer membrane to varying concentrations of AMP (**7**). (B) The gate–source potential change of the ISFET device modified with GMP-imprinted acrylamide–acrylamidephenylboronic acid copolymer upon: (a) the sensing of varying concentrations of GMP (**8**); (b),(c) the sensing of varying concentrations of AMP (**7**) and CMP (**9**); (d) the response of the ISFET modified with the non-imprinted membrane to varying concentrations of GMP (**8**). (C) The gate–source potential changes of the ISFET modified with the CMP-imprinted acrylamide–acrylamidephenylboronic acid copolymer membrane upon: (a) the sensing of varying concentrations of CMP (**9**); (b),(c) the sensing of varying concentrations of AMP (**7**) and GMP (**8**), respectively; (d) the response of the ISFET modified with the non-imprinted membrane to varying concentrations of CMP (**9**).

we imprinted $^{14}CH_3CO_2H$ in the TiO_2 membrane associated with the ISFET device, by a procedure similar to that outlined for the different acids. We find that ca. 65–70% of the radioactive counts associated with the film are washed-off. The immobilization of the imprinted TiO_2 film on the gate interface results in the spreading of the imprinted membrane also on parts of the encapsulated source and drain electrodes. The imprinted membrane parts that are not associated with the gate are inactive in the sensing surface. Accordingly, we have immobilized a polymerized TiO_2 film of the imprinting solution on an Au-quartz-crystal. By following the crystal frequency changes we were able to estimate the total weight of the membrane. Thus, the radioactive counts measured upon the release of $^{14}CH_3CO_2H$ correspond to the escape of the imprinted acid from the total TiO_2 volume. Knowing the gate area ($20\times700\ \mu m^2$) and the membrane thickness, ca. 85 μm, we estimate the active membrane weight in the sensing surface. Using the respective radioactive counts, we estimate that ca. 3.7×10^{18} imprinted sites per gram are associated with the TiO_2 membrane. It should be noted that since the radioactive label is acetic acid, the number of imprinted recognition sites in the sensing interface might be considered only as a rough estimate of the number of recognition sensing sites of the other acids described in this study.

A further direction to generate an imprinted specific

membrane on a field-effect transistor involved the application of an imprinted phenyl boronic acid acrylamide–acrylamide copolymer as an active sensing interface for nucleotides on the ISFET device. Boronic acid ligands bind strongly and reversibly with diols, Eq. (4). The association properties of the boronic acid ligand were used to develop sensing ligating materials for the optical detection of sugars[26] and for the development of gelating materials that undergo controlled sol–gel transitions in the presence of sugars.[27] Crosslinked polymers composed of 2-hydroxyethylmethyacrylate and 4-vinylphenylboronic acid, were used as functional hydrogels for the adsorption of nucleotides.[28] Similarly, layered assemblies consisting of the polyanionic acrylic acid–acrylamide boronic acid and the polycationic polydimethyl diallylammonium chloride were employed for the microgravimetric analysis of adenosine-5′-monophosphate, AMP, and adenosine-5-triphosphate, ATP, using a QCM.[29] Also, the swelling of an acrylamide–acrylamidephenylboronic acid copolymer film on surfaces upon interaction with glucose was used for the sensing of glucose.[30] Surface plasmon resonance spectroscopy, Faradaic impedance spectroscopy, and microgravimetric quartz-crystal microbalance experiments were used as optical and electronic transduction means for the sensing of glucose by the hydrogel. The boronic acid ligand was extensively used for the imprinting of molecular recognition sites in polymers for the specific adsorption and separation of sugars. For example, imprinted sites for phenyl-α-D-mannopyranoside were generated in acrylic acid-4-vinylphenylboronic acid copolymer.[31] The development of specific sensing interfaces for nucleotides, and eventually nucleic acids, is of fundamental and practical interest. Tailoring of specific recognition sites for nucleotides would enable us to define the recognition interactions in the binding cavities at the molecular level, whereas such specific binding interfaces could be effective nucleotide sensing matrices, e.g. for DNA or RNA sequencing. Only a few reports attempted to develop imprinted polymers for nucleotides. Ethylene glycol dimethacrylate–methacrylic acid copolymers were used to imprint the pyrimidine/purine bases appearing in nucleic acids using hydrogen-bond recognition interactions.[32] Functional fluorophore-labeled imprinted polymers for the cyclic adenosine 3′,5′-monophosphate, cAMP, were prepared and the fluorescence quenching of the label by the bound nucleotide was used to probe cAMP.[33] A further attempt to imprint molecular recognition sites for adenosine monophosphate, AMP, was reported using a layered array composed of an anionic acrylic acid–acrylamidephenylboronic acid, acting as template layer for AMP and a cationic polymer layer that functions as a capping interface for bound AMP.[34] Nonetheless, in none of these studies the specific imprint and sensing of the DNA bases has been demonstrated. The association of *cis*-diols to the boronic-acid ligand charges the polymer, Eq. (4). This suggests that the assembly of a boronic acid polymer and specifically an imprinted boronic acid polymer, on the gate surface of the ISFET could yield a functional interface that controls the gate potential upon binding of the host–substrate to the polymer matrix (charging of the polymer). Here we describe the novel imprinting of the three ribose-functionalized nucleotide bases in an acrylamide–acrylamidephenylboronic acid copolymer assembled on the ISFET device.

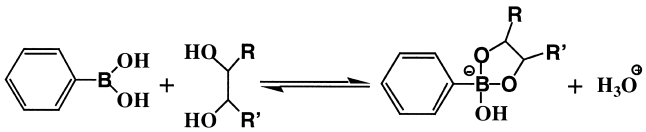

(4)

An acrylamide–acrylamidephenylboronic acid crosslinked copolymer was in situ polymerized in the presence of the respective nucleotide AMP (**7**), guanosine 5′-monophosphate GMP (**8**) or cytosine 5′-monophosphate CMP (**9**), on the gate interface of the ISFET. The concept of imprinting of the molecular recognition sites is schematically shown in Scheme 2 for AMP (**7**). The formation of the boronic acid ribose unit complex provides the primary template for the generation of the imprinted cavity. The secondary association of acrylamide polymer units to the adenine or phosphate sites through hydrogen bonds provides the mechanism for rigidifying the molecular recognition contour in the polymer, and for the orientation of the respective functional groups for binding of the substrate. Rinsing of the crosslinked polymer with ammonia is then expected to deplete the imprinted substrate, and to yield imprinted membranes for the respective nucleotides on the gate surface.

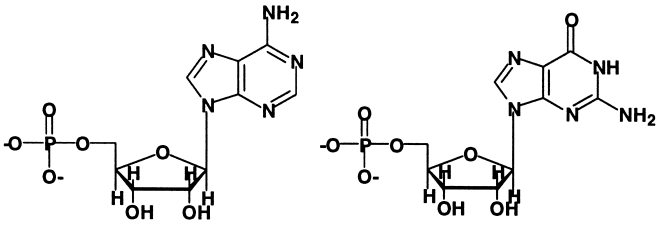

AMP (7) **GMP (8)**

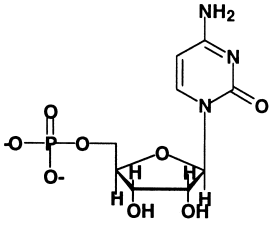

CMP (9)

Fig. 5(A), curve (a), shows the gate–source potential of the ISFET device that includes imprinted sites for AMP, upon sensing of variable concentrations of AMP (**7**). The substrate is detected in the concentration range of 3.0×10^{-5} to 5×10^{-3} M with a sensitivity that corresponds to 14.0 mV/dec and a detection limit of 1.5×10^{-5} M. Fig. 5(A), curves (b) and (c), show the responses of the AMP-imprinted ISFET device upon the sensing of GMP and CMP, respectively. Clearly, the responses of the device to the non-imprinted substrates are substantially lower. For example, GMP and CMP are detected only at concentrations higher than 10^{-3} M with the poor sensitivity of 4 mV/dec. Fig. 5(A), curve (d), shows the response of a non-imprinted acrylamide–acrylamidephenylboronic acid membrane in the presence of AMP. Clearly, the polymer sensitivity is only 5 mV/dec in the concentration range of 10^{-4}–10^{-3} M.

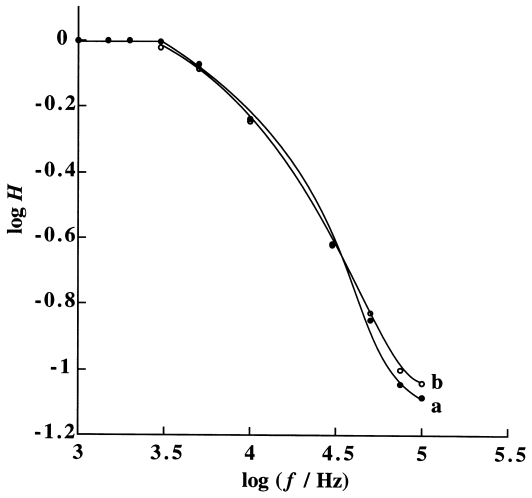

Figure 6. Transconductance curves of: (a) the bare ISFET, and (b) the acrylamide–acrylamidephenylboronic acid copolymer film-functionalized ISFET device. Using the corresponding time-constants, τ_1 and τ_2 (and Eqs. (1)–(3)) we estimate the film thickness to be 360±10 Å.

Fig. 5(B), curve (a) shows the gate–source potential of the ISFET device that includes the GMP-imprinted copolymer membrane on the gate upon sensing varying concentrations of (**8**). The GMP is detected by this functional interface in the concentration range of 4×10^{-5} to 2×10^{-3} M with a sensitivity of 17.0 mV/dec and a detection limit of 1.5×10^{-5} M. Fig. 5(B), curves (b) and (c), shows the responses of the GMP-imprinted ISFET device in the presence of AMP and CMP, respectively. It is seen that GMP-imprinted membrane-functionalized ISFET device enables the sensing of (**7**) and (**9**) in the concentration ranges of 2×10^{-4} to 7×10^{-3} M ((**7**) and (**9**), respectively) with the slope of the linear segments of 5.0 mV/dec. The lower detection limits for the sensing of (**7**) and (**9**) correspond to 6.0×10^{-4} and 8.0×10^{-4} M, respectively. Fig. 5(B), curve (d), shows the response of the non-imprinted polymer-functionalized-device in the presence of added GMP. The device reveals only minute response in the concentration range of 10^{-4}–10^{-3} M with the sensitivity of 6 mV/dec. Fig. 5(C), curve (a), shows the gate–source potentials of the CMP-imprinted polymer-functionalized-ISFET upon analysis of CMP (**9**). The imprinted substrate is detected in the concentration range of 2×10^{-6}–5×10^{-4} M, a sensitivity of 17.0 mV/dec and a detection limit that corresponds to 8×10^{-7} M. Fig. 5(C), curves (b) and (c), shows the responses of the CMP-imprinted device upon interaction with AMP on GMP. Clearly, the CMP-imprinted device responds to the presence of (**8**) in the entire concentration range of 10^{-6}–10^{-2} M with a minute sensitivity that corresponds to 2 mV/dec. At the same time, the (**9**)-imprinted polymer-based ISFET is entirely insensitive to the presence of AMP, which can be attributed to the substantially larger dimensions of this substrate. Fig. 5(C), curve (d) shows the response of the non-imprinted-polymer-functionalized FET device upon interaction with CMP (**9**). The response of the non-imprinted device is 5 mV/dec in the concentration range of 10^{-5}–10^{-4} M.

This set of experiments applying the nucleotide-imprinted polymers in analyzing the respective imprinted substrates, and the complementary control experiments, reveal some important conclusions on the activity and selectivity of the functional imprinted polymer membranes: (i) imprinting of molecular recognition sites in the polymer membranes enhances the detection limits and the sensitivities of the sensing interfaces. This is probably due to the higher binding capacities of the imprinted membranes for the imprinted substrates and (ii) the imprinted polymer membranes reveal structural selectivity towards the sensing of the imprinted substrates. This suggests that the imprinting process leads to well defined molecular contours that include the boronic-acid ligand and H-bonding anchoring sites in appropriately aligned positions in the tailored cavities.

To further characterize the sensing membrane on the gate surface, its thickness was evaluated by impedometric measurements.[23–25] Fig. 6 shows the transconductance functions of the system at variable applied frequencies. From these plots the time-constant τ_1 (Eq. (1)) and τ_2 (Eq. (2)) were extracted. Using these time-constants, the resistance of the polymer membrane, R_{mem}, and its capacitance, C_{mem}, were determined. The value C_{ox} corresponds to the capacitance of the Al_2O_3 gate on which the polymer film is assembled. From these values the polymer film thickness, δ_{mem}, was determined using Eq. (3), where ϵ_o is the dielectric constant of the vacuum ($\epsilon_o=8.85\times10^{-12}$ F/m), and A is the gate area. The polymer film thickness is estimated to be 360±10 Å.

2. Conclusions and perspectives

The present study has addressed the imprinting of molecular recognition sites in inorganic TiO_2 films, and acrylamide–acrylamidephenylboronic acid crosslinked copolymer membranes, associated with ISFET devices. Molecular structures of carboxylic acids, e.g. 4-chlorophenoxyacetic acid (**1**), 2,4-dichlorophenoxyacetic acid (**2**), fumaric acid (**3**), and maleic acid (**4**), were imprinted in TiO_2 films assembled on the ISFET gate interface. The imprinted sites reveal high specificity, and substrates structurally-related to the imprinted compounds, are fully differentiated by the imprinted membranes. The specificity of the imprinted sites originates from the complementary structural fitting and ligation of the carboxylic acid residues to the Ti(IV)–OH, of the host carboxylic acids to the imprinted cavities. The acrylamide–acrylamidephenylboronic acid copolymer provides a functional polymer for the imprinting of binding sites for nucleotides, e.g. AMP (**7**), GMP (**8**), and CMP (**9**). The charging of the polymer membrane upon the binding of the nucleotides controls the ISFET gate potential and enables the sensing of the respective nucleotides. Significant selectivity of the imprinted sites is observed, although no attempt to enhance the response and specificity was made. In all of the systems described in the study, the response-times of the sensor devices was ca. 5 min. The specificity of the imprinted sites in the organic polymer is attributed to the cooperative binding interactions between the imprinted substrate and the polymer consisting of the boronic acid ligand as the ligating site for the nucleotides ribose units and complementary H-bonds between the acrylamide units and the nucleotide. The multi-site binding cavity generates a rigid structural contour for the binding of the imprinted

nucleotide. We may expect that the specificity of the imprinted sites may be enhanced by further rigidification of the recognition sites by the optimization of the crosslinking degree of the polymer.

3. Experimental

3.1. Materials

The monomer 3-acrylamidenphenylboronic acid was synthesized according to the published procedure.[35] All other chemicals were purchased from Aldrich or Sigma and were used as supplied. Ultra pure water from Seralpur PRO 90 CN was used throughout the experiments.

3.2. Preparation of ISFET

A solution of Ti(IV) butoxide in ethanol/toluene (1:1) mixture was treated with the respective carboxylic acid. The resulting mixture, which included the Ti(IV) butoxide–carboxylate complex, was deposited onto the gate surface. The sol–gel polymerization of the mixture on the gate resulted in a thin TiO_2 film with the embedded carboxylate. The gate of the ISFET was functionalized by placing a 0.4 μL drop of the Ti(IV) butoxide–carboxylate complex solution on the gate. The system was then allowed to dry in an oven (Eurotherm) at 40°C overnight. The resulting modified chip was thoroughly rinsed with toluene and then with the working buffer solution. Treatment of the film with ammonia solution (1% v/v for 2 min) resulted in the elimination of the carboxylate and the formation of imprinted molecular sites for the respective acid within the TiO_2 film. The ISFET was then treated with ammonia solution (1% v/v for 2 min) and again with the working buffer.

For the preparation of the imprinted polymer membrane for the nucleotides, a mixture, consisting of acrylamide (1.82 M), 3-(acrylamido)phenylboronic acid (0.18 M), *N*,*N*′-methylenebisacrylamide (0.04 M), *N*,*N*,*N*′,*N*′-tetramethylethylenediamine (0.25 mL 10% v/v) and the respective nucleotide (0.1 M) were dissolved in 1 mL of a freshly prepared solution of phosphate saline buffer (PBS), (0.01 M sodium phosphate+NaCl (0.14 M), pH=7.2). The initiator of the polymerization ammonium persulfate (0.22 M, 0.1 mL) was added to the monomer solution just before placing an 0.4 μL drop of the mixture on the gate interface. The resulting modified chip was dried under air for 3 h. The ISFET was then rinsed with NH_3 solution (1% v/v, for 2 min) to eliminate the nucleotide from the polymer film. This procedure led to the elimination of the nucleotide and the formation of the imprinted membrane for the respective nucleotide. The resulting functionalized ISFET was thoroughly rinsed with PBS, and used for the analytical measurements.

3.3. Measurements

ISFET devices with Al_2O_3 or SiO_2 gate interfaces (20×700 μm^2, IMT, Neuchâtel, Switzerland) and an Ag/AgCl reference electrode were used in all the experiments. The chip modified by the respective molecularly imprinted film was immersed in the working cell filled with PBS (0.8 mL, pH=7.2) and variable concentrations of the respective substrate (carboxylic acid or nucleotide). The output signal between the source of the ISFET and the reference electrode was recorded using a semiconductor parameter analyzer (HP 4155 B). Each measurement was performed for 15 min with a time interval of 2 min. The system configuration enabled the measurements of the source–gate voltage (V_{gs}), while the drain current (I_d) or the source-drain voltage (V_{ds}) remained constant (I_d= 100 μA and V_{ds}=1.5 V). The difference in the V_{gs} for the ISFET modified by the respective films with or without the embedded substrate residue was plotted versus the substrate concentration. All the experiments were carried out at ambient temperature and without stirring, in order to simulate real conditions of possible future in vivo applications. Reproducibility of the measurements was ±2 mV in a number of experiments (n=5).

3.4. Evaluation of the polymer film thickness

The thickness of the TiO_2-imprinted film and the acrylamide-acrylamidophenylboronate copolymer membrane were evaluated by impedance spectroscopy measurements on the ISFET device.[23] The electronic circuit and instruments used to follow the impedance properties of the modified ISFET, and the conditions under which the experiments were carried out were described elsewhere.[24] To determine the transconductance transfer functions, the output potential, V_{out}, at variable frequencies from 1 Hz to 100 KHz, was related to the imaginary impedance, Z_{im}. The values of the output potentials corresponding to Z_{im} were normalized at 1 Hz to give the respective transfer function.[24]

Acknowledgements

This research is supported by the Israel Ministry of Science as an Infrastructure project in Material Science. I. W. acknowledges the Max Planck Research Award for International Cooperation. M. L. Acknowledges the support of the Clore Israel Foundation Scholars Programme.

References

1. (a) Lanza, F.; Sellergren, B. *Anal. Chem.* **1999**, *71*, 2092–2096. (b) Panasyuk, T. L.; Mirsky, V. M.; Piletsky, S. A.; Wolfbeis, O. S. *Anal. Chem.* **1999**, *71*, 4609–4613. (c) Dickert, F. L.; Tortschanoff, M.; Bulst, W. E.; Fischerauer, G. *Anal. Chem.* **1999**, *71*, 4559–4563.
2. (a) Katz, A.; Davis, M. E. *Nature (London)* **2000**, *403*, 286–289. (b) Glad, M.; Norrlöw, D.; Sellergren, B.; Siegbahn, N.; Mosbach, K. *J. Chromatogr.* **1985**, *347*, 11–15. (c) Markowitz, M. A.; Kust, P. R.; Deng, G.; Schoen, P. E.; Dordick, J. S.; Clark, D. S.; Gaber, B. P. *Langmuir* **2000**, *16*, 1759–1765.
3. (a) Mosbach, K.; Ramström, O. *Biotechnology* **1996**, *14*, 163–170. (b) Klein, J. U.; Whitcombe, M. J.; Mulholland, F.; Vulfson, E. N. *Angew. Chem., Int. Ed. Engl.* **1999**, *38*, 2057–2060. (c) Yilmaz, E.; Mosbach, K.; Haupt, K. *Anal. Commun.* **1999**, *71*, 285–287.

4. (a) Sellergren, B.; Shea, K. J. *J. Chromatogr., A* **1995**, *690*, 29–39. (b) Andersson, L. I.; Müller, R.; Vlatakis, G.; Mosbach, K. *Proc. Natl. Acad. Sci. USA* **1995**, *92*, 4788–4792. (c) Lee, C. W.; Ichinose, I.; Kunitake, T. *Langmuir* **1998**, *14*, 2857–2863.
5. (a) Wulff, G. *Angew. Chem., Int. Ed. Engl.* **1995**, *34*, 1812–1832. (b) Wulff, G.; Gross, T.; Schönfeld, R. *Angew. Chem., Int. Ed. Engl.* **1997**, *36*, 1962–1964. (c) Piletsky, S. A.; Piletskaya, E. V.; Chen, B.; Karim, K.; Weston, D.; Barrett, G.; Lowe, P.; Turner, A. P. F. *Anal. Chem.* **2000**, *72*, 4381–4385.
6. (a) Malik, S.; Johnson, R. D.; Arnold, F. H. *J. Am. Chem. Soc.* **1994**, *116*, 8902–8903. (b) Hart, B. R.; Shea, K. J. *J. Am. Chem. Soc.* **2001**, *123*, 2072–2073.
7. (a) Dai, S.; Shin, Y.; Barnes, C. E.; Toth, L. M. *Chem. Mater.* **1997**, *9*, 2521–2525. (b) Sasaki, D. Y.; Alam, T. M. *Chem. Mater.* **2000**, *12*, 1400–1407. (c) Makote, R.; Collinson, M. M. *Chem. Mater.* **1998**, *10*, 2440–2445.
8. Lee, S. W.; Ichinose, I.; Kunitake, T. *Chem. Lett.* **1998**, *12*, 1193–1194.
9. (a) Matsui, J.; Nicholls, I. A.; Takeuchi, T. *Tetrahedron: Asymmetry* **1996**, *7*, 1357–1361. (b) Ramström, O.; Nicholls, I. A.; Mosbach, K. *Tetrahedron: Asymmetry* **1994**, *5*, 649–656. (c) Schweitz, L.; Andersson, L. I.; Nilsson, S. *Anal. Chem.* **1997**, *69*, 1179–1183.
10. (a) Nilsson, K. G. I.; Lindell, J.; Norrlöw, O.; Sellergren, B. *J. Chromatogr., A* **1994**, *680*, 57–61. (b) Vallano, P. T.; Remcho, V. T. *J. Chromatogr., A* **2000**, *887*, 125–135.
11. (a) Mayes, A. G.; Andersson, L. I.; Mosbach, K. *Anal. Biochem.* **1994**, *222*, 483–488. (b) Kempe, M. *Anal. Chem.* **1996**, *68*, 1948–1953. (c) Kriz, D.; Berggren-Kriz, C.; Andersson, L. I.; Mosbach, K. *Anal. Chem.* **1994**, *66*, 2636–2639. (d) Quaglia, M.; Chenon, K.; Hall, A. J.; De Lorenzi, E.; Sellergren, B. *J. Am. Chem. Soc.* **2001**, *123*, 2146–2154.
12. (a) Lin, J. M.; Nakagama, T.; Uchiyama, K.; Hobo, T. *Chromatographia* **1996**, *43*, 585–591. (b) Schweitz, L.; Spégel, P.; Nilsson, S. *Analyst* **2000**, *125*, 1899–1901.
13. (a) Brunkan, N. M.; Gagne, M. R. *J. Am. Chem. Soc.* **2000**, *122*, 6217–6225. (b) Whitcombe, M. J.; Alexander, C.; Vulfson, E. N. *Synlett* **2000**, 911–923.
14. (a) Hedborg, E.; Winquist, F.; Lundström, I.; Andersson, L. I.; Mosbach, K. *Sens. Actuators, A* **1993**, *37–38*, 796–799. (b) Dickert, F. L.; Thierer, S. *Adv. Mater.* **1996**, *8*, 987–990. (c) Piletsky, S. A.; Piletskaya, E. V.; Panasyuk, T. L.; El'skaya, A. V.; Levi, R.; Karube, I.; Wulff, G. *Macromolecules* **1998**, *31*, 2137–2140.
15. (a) Wang, W.; Gao, S.; Wang, B. *Org. Lett.* **1999**, *1*, 1209–1212. (b) Liao, Y.; Wang, W.; Wang, B. H. *Bioorg. Chem.* **1999**, *27*, 463–476.
16. (a) Liang, C. D.; Peng, H.; Bao, X. Y.; Nie, L. H.; Yao, S. Z. *Analyst* **1999**, *124*, 1781–1785. (b) Ji, H. S.; McNiven, S.; Ikebukuro, K.; Karube, I. *Anal. Chim. Acta* **1999**, *390*, 93–100. (c) Haupt, K.; Noworyta, K.; Kutner, W. *Anal. Commun.* **1999**, *36*, 391–393.
17. (a) Kugimiya, A.; Takeuchi, T. *Electroanalysis* **1999**, *11*, 1158–1160. (b) Malitesta, C.; Losito, I.; Zambonin, P. G. *Anal. Chem.* **1999**, *71*, 1366–1370. (c) Dickert, F. L.; Forth, P.; Lieberzeit, P.; Tortschanoff, M. *Fresenius J. Anal. Chem.* **1998**, *360*, 759–762.
18. Lahav, M.; Katz, E.; Doron, A.; Patolsky, F.; Willner, I. *J. Am. Chem. Soc.* **1999**, *121*, 862–863.
19. Mirsky, V. M.; Hirsch, T.; Piletsky, S. A.; Wolfbeis, O. S. *Angew. Chem., Int. Ed. Engl.* **1999**, *38*, 1108–1110.
20. Lahav, M.; Kharitonov, A. B.; Katz, O.; Kunitake, T.; Willner, I. *Anal. Chem.* **2001**, *73*, 720–723.
21. (a) Haupt, K.; Mayer, A. G.; Mosbach, K. *Anal. Chem.* **1998**, *70*, 3936–3939. (b) Kröger, S.; Turner, A. P. F.; Mosbach, K.; Haupt, K. *Anal. Chem.* **1999**, *71*, 3698–3702. (c) Jakusch, M.; Janotta, M.; Mizaikoff, B.; Mosbach, K.; Haupt, K. *Anal. Chem.* **1999**, *71*, 4786–4791. (d) Surugui, I.; Ye, L.; Yilmaz, E.; Dzgoev, A.; Danielsson, B.; Mosbach, K.; Haupt, K. *Analyst* **2000**, *125*, 13–16.
22. Haupt, K. *Analyst* **2001**, *126*, 747–756.
23. (a) Friebe, A.; Lisdat, F.; Moritz, W. *Sens. Mater.* **1993**, *5*, 65–78. (b) Antonisse, M. M. G.; Snellink-Rüel, B. H. M.; Lugtenberg, R. J. W.; Engbersen, J. F. J.; van den Berg, A.; Reinhoudt, D. N. *Anal. Chem.* **2000**, *72*, 343–348.
24. Kharitonov, A. B.; Wasserman, J.; Katz, E.; Willner, I. *J. Phys. Chem. B* **2001**, *105*, 4205–4213.
25. Lahav, M.; Kharitonov, A. B.; Willner, I. *Chem. Eur. J.* **2001**, *7*, 3982–3997.
26. (a) James, T. D.; Sandanayake, K. R. A. S.; Shinkai, S. *Nature* **1995**, *374*, 345–347. (b) Yoon, J.; Czarnik, A. W. *J. Am. Chem. Soc.* **1992**, *114*, 5874–5875.
27. James, T. D.; Murata, K.; Harada, T.; Ueda, K.; Shinkai, S. *Chem. Lett.* **1994**, 273–276.
28. Özdemir, A.; Tuncel, A. *J. Appl. Polym. Sci.* **2000**, *78*, 268–277.
29. Kanekiyo, Y.; Sano, M.; Iguchi, R.; Shinkai, S. *J. Polym. Sci. A* **2000**, *38*, 1302–1310.
30. Gabai, R.; Sallacan, N.; Chegel, V.; Bourenko, T.; Katz, E.; Willner, I. *J. Phys. Chem. B.* **2001**, *105*, 8196–8202.
31. (a) Wulff, G.; Poll, H. G.; Minarik, M. *J. Liq. Chromatogr.* **1986**, *9*, 385–405. (b) Wulff, G.; Minarik, M. *HRG&CC J. High Resolut. Chromatogr., Chromatogr. Commun.* **1986**, *9*, 2987–3000
32. Spivak, D. A.; Shea, K. J. *Macromolecules* **1998**, *31*, 2160–2165.
33. Turcewitch, P.; Wandelt, B.; Darling, G. D.; Powell, W. S. *Anal. Chem.* **1998**, *70*, 2025–2030.
34. Kanekiyo, Y.; Ono, Y.; Inone, K.; Sano, M.; Shinkai, S. *J. Chem. Soc., Perkin Trans. 2* **1999**, 557–561.
35. Kitano, S.; Koyama, Y.; Kataoka, K.; Okano, T.; Sakurai, Y. *J. Controlled Release* **1992**, *19*, 162–170.